

KEYWORDS: iodine behavior, chemical thermodynamic modeling, Knudsen-cell effusion

CHEMICAL SPECIATION OF IODINE SOURCE TERM TO CONTAINMENT

JOANNA McFARLANE*† Atomic Energy of Canada Limited
Whiteshell Laboratories, Containment Analysis Branch
Pinawa, Manitoba R0E 1L0, Canada

JUNGSOOK C. WREN and ROBERT J. LEMIRE
Atomic Energy of Canada Limited, Chalk River Laboratories
Fuel Safety Branch, Chalk River, Ontario K0J 1J0, Canada

Received August 1, 2001

Accepted for Publication December 5, 2001

Iodine species released into a reactor containment building following a loss-of-coolant accident is determined by the relative timing and quantity of iodine and other fission products released from the fuel, chemical thermodynamics in the fuel channel, and reaction kinetics in cooler regions of the heat transport system (HTS). Iodine speciation along the transport path from the fuel to cooler regions of the HTS and into containment is evaluated using chemical thermodynamics calculations, leading to a prediction of the volatile iodine mole fraction that theoretically would enter containment. Sensitivities to a decrease in the cesium-to-iodine ratio, a decrease in iodine concentration in the coolant, and an increase in oxygen partial pressure are tested. The role of the presence of other elements, namely, molybdenum, tellurium, uranium, and lithium, are also evaluated. Under

most conditions, the mole fraction of iodine entering containment in volatile form is found to be <0.1%. There are circumstances, however, when cesium iodide can be destabilized by a low cesium-to-molybdenum ratio in an oxidizing atmosphere such as steam. To further explore this situation and to validate the code, chemical equilibrium calculations are also compared to earlier Knudsen-cell experimental studies of the interaction of cesium, iodine, molybdenum, and uranium. In these experiments, the partial pressures of cesium molybdate and elemental iodine are measured as a function of temperature over the range 1100 to 1500 K. The calculated Cs_2MoO_4 vapor pressures agree with the experimental results within an order of magnitude at temperatures up to 1200 K; and between 770 and 1150 K, the agreement is within a factor of 2 to 5 depending on the chemical system.

I. INTRODUCTION

It is generally recognized that radioiodine is potentially one of the most hazardous fission products that could be released following a loss-of-coolant accident (LOCA). The reasons why radioiodine is so potentially hazardous are as follows: it has a large inventory in irradiated nuclear fuel; its isotope of greatest radiological significance, ^{131}I , has a half-life of 8.04 days; it has a complex chemistry that may lead to the formation of volatile species; and it can cause hazardous biological

effects. It is therefore important to be able to predict iodine release from containment to the external atmosphere and hence public dose for postulated accidents.

Iodine speciation as it is initially released into the containment atmosphere from the fuel after passing through the heat transport system (HTS) is a key input to reactor accident consequence analysis. Iodine transport behavior inside containment and its form of release to the outside atmosphere strongly depend on its speciation. For safety analysis purposes, iodine in containment is divided into airborne and nonairborne species, and airborne species are divided into water droplets (aerosols) and gaseous species. The objective of the current work is to theoretically determine iodine speciation in the HTS and as a consequence the iodine speciation introduced to containment following a postulated

*Current address: Oak Ridge National Laboratory, Box 2008, Oak Ridge, Tennessee 37831.

†E-mail: mcfarlanej@ornl.gov

accident.^a From this evaluation, the time-dependent fractions of iodine entering containment in aerosol and gaseous forms can be predicted.

Fuel temperature, fuel power history and transient behavior, and fuel environment (e.g., steam, hydrogen, air, and water) determine the amounts of fission products released from the fuel, their relative ratios, and the timing of their release—for instance, the rates of diffusion of iodine and other fission products to the grain boundaries and gap increase with fuel temperature and fuel oxidation.¹ Once released from the fuel, fission product speciation will vary because of temperature gradients along the transport path from the fuel to cooler regions of the HTS and into containment.

Various chemical kinetic calculations have shown that thermodynamic equilibrium of gap inventory fission products released from fuel is rapidly attained (in <0.1 s) at temperatures >1000 K (Refs. 2 and 3). The kinetic behavior of iodine and cesium has been modeled for the Canada Deuterium Uranium reactor (CANDU)^b HTS at 1.2 MPa, using 17 chemical species, containing iodine, cesium, hydrogen, and oxygen, accounting for the 152 reactions among them.² The final steady-state concentrations of iodine and cesium species agreed well with concentrations obtained from equilibrium calculations. At high temperatures, the “volatile”^c forms of iodine (HI, I, and I₂) are important, as predicted by thermodynamic equilibrium calculations (see Sec. III); however, at temperatures <1000 K, CsI is the most stable iodine species, and all the other iodine species comprise a very small fraction.

The kinetic calculations showed that at 1000 K, conversion of released cesium and iodine to CsI and CsOH is effectively complete within 0.01 s. A three-node calculation was performed, with residence times of 0.28 s at each of 1500, 1000, and 750 K. The results show very rapid formation of CsI and CsOH: in ~ 0.001 s for high concentrations of CsI ($8 \text{ mol} \cdot \text{m}^{-3}$ cesium, $0.8 \text{ mol} \cdot \text{m}^{-3}$ iodine) in the 1500 K node, and in 0.01 s for lower concentrations of CsI ($0.08 \text{ mol} \cdot \text{m}^{-3}$ cesium, $0.008 \text{ mol} \cdot \text{m}^{-3}$

iodine) even in the 1000 K node. In the 750 K node, the system takes $>10^3$ s to reach equilibrium. The HI and I disappear in 0.1 s, except for low concentrations of cesium and iodine. Changing the steam pressure within a range of a factor of 5 does not significantly affect the result. The kinetic calculations indicate that even during rapid cooling from temperatures near 2273 K to 1500 or 1000 K, CsI and CsOH are formed. Kinetic calculations were also done as one component of mixed kinetic/thermodynamic calculations of light water reactor (LWR) accident scenarios.³ The system of reactions was much simpler than that described in Ref. 2, with only 20 reactions being considered. Detail on equilibration times was provided for one case, with equilibrium being reached rapidly at 1180 K, but not at 907 K.

In summary, kinetics calculations have shown that at temperatures >1000 K, progress to equilibrium occurs in less time than the residence time in the channel (>0.4 s for steam at 1000 K and 101.325 kPa). Thus, speciation at temperatures >1000 K can be determined by thermodynamic equilibrium calculations, which have been used to model the speciation of fission products in the fuel and in the channel under prototypical reactor accident conditions.⁴ In this paper, these calculations are compared to Knudsen-cell investigations of the volatility of mixtures of CsI, Mo or MoO₂, Cs₂MoO₄, and UO_{2+x} (Ref. 5), to assess the ability of the CHMWRK computer code to model chemical systems involving cesium, molybdenum, and iodine.

Chemical equilibrium calculations are also used to calculate iodine speciation in the HTS to provide the initial fraction of gaseous species and aerosols released into the containment atmosphere. Fission products would likely be exposed to temperatures <1000 K before they are released from the HTS into containment, where temperatures are expected to be <450 K. However, because the fraction of volatile iodine is greater at higher temperatures, it can be assumed that thermodynamic equilibrium calculations at 1000 K will give an upper bound to the amount of volatile iodine released to containment in the gas phase.

Assuming that reaction kinetics are fast in the HTS and that chemical equilibrium is rapidly attained, cesium and iodine speciation at a given temperature depend on the amounts of all elements present—primarily cesium, iodine, hydrogen, and oxygen^d—and the thermodynamic properties of all their chemical compounds. Confidence in the calculated mole fraction of iodine species released from the HTS into containment thus depends on uncertainties within the thermodynamic database, the relative amounts of elements involved as determined by the release rates from the fuel, and the proper identification of

^aIodine chemistry and transport in containment is a complex topic in its own right and thus is not addressed in this document. Comprehensive reviews on this topic can be found in the following publications: J. C. WREN and J. M. BALL, “LIRIC 3.2 An Updated Model for Iodine Behaviour in the Presence of Organic Impurities,” *Radiat. Phys. Chem.*, **60**, 577 (2001); J. C. WREN, J. M. BALL, and G. A. GLOWA, “The Chemistry of Iodine in Containment,” *Nucl. Technol.*, **129**, 297 (2000).

^bCanada Deuterium Uranium is a registered trademark of Atomic Energy of Canada Limited.

^cIn this documentation, the term “volatile (species)” refers to the species that would be in gaseous form under containment building conditions typical of a reactor accident (i.e., <450 K). Gaseous species in containment are of particular concern because of their huge mobility and hence the large potential for release to the outside atmosphere.

^dSilver was not included in these calculations because it is not available for reaction with iodine in CANDU reactors. When present, it will dominate iodine chemistry, both in the HTS and in containment.⁶

all potentially volatile species. Sensitivities of the calculated results to variations in physical input variables—such as temperature, pressure, and mole fraction—were performed in order to estimate the overall uncertainty in the results.

II. THERMODYNAMIC CALCULATIONS

Because thermodynamic equilibrium is rapidly attained, one can follow thermodynamic equilibrium as a function of temperature to determine the change in iodine speciation as the fission products travel through the temperature gradient, down to 1000 K, in the HTS. The equilibrium speciation calculations were performed using the CHMWRK chemical thermodynamic equilibrium code, which computes the minimum Gibbs function for a system using the Villars-Cruise-Smith algorithm for given temperature, pressure/volume, and elemental abundance constraints.⁷ Components of the gas phase are treated as an ideal mixture, whereas condensed phases are treated as though they act independently of one another. There is limited ability to handle nonstoichiometric alloys, such as that between zirconium and tin, but these were not used in this series of calculations.

II.A. The CHMWRK Thermodynamic Database

Thermodynamic equilibrium calculations require the Gibbs energy of formation $\Delta_f G^\circ$ and standard entropy S° , at 298.15 K, and the temperature-dependent Gibbs energy function $\Phi(T)$, for each element or compound. For any species,

$$\Phi(T) = -\frac{[G^\circ(T) - H(298.15)]}{T} \quad (1)$$

is defined in terms of the species Gibbs energy $G(T)$ and enthalpy H . The temperature dependence of $\Phi(T)$ was fit to a six-parameter expression in X , where $X = 10^{-4} \cdot T$:

$$\Phi(T) = A_0 + A_{\ln} \ln(X) + A_{-2} X^{-2} + A_{-1} X^{-1} + A_1 X + A_2 X^2 + A_3 X^3 \quad (2)$$

A complete publication of the database is not available, so this section gives the reference information for the database. The species used in the calculations are also tabulated in Table I. The phases are designated as (s) solid, (c) condensed (i.e., solid or liquid), (g) gas, or (ss) solid solution.

The reference information for the database is as follows.

O(g), O₂(g), H(g), H₂(g), OH(g), H₂O(g), I(g), I₂(g), HI(g), Cs(c), and Cs(g)

The values for O(g), O₂(g), H(g), H₂(g), OH(g), H₂O(g), I(g), I₂(g), HI(g), Cs(c), and Cs(g) are based

on those of Cordfunke and Konings,⁸ and come from the CODATA review⁹ and a 1989 assessment by Gurvich et al.¹⁰

Cs₂(g), CsI(c), CsI(g), Cs₂I₂(g), Mo(c), Mo(g), Mo₂(g), MoO(g), MoO₂(s), MoO₂(g), MoO₃(c), MoO₃(g), H₂MoO₄(g), and Cs₂MoO₄(c)

Values for Cs₂(g), CsI(c), CsI(g), Cs₂I₂(g), Mo(c), Mo(g), Mo₂(g), MoO(g), MoO₂(s), MoO₂(g), MoO₃(c), MoO₃(g), H₂MoO₄(g), and Cs₂MoO₄(c) are taken from Cordfunke and Konings.⁸

Mo₂O₆(g), Mo₃O₉(g), Mo₄O₁₂(g), and Mo₅O₁₅(g)

The database values for Mo₂O₆(g), Mo₃O₉(g), Mo₄O₁₂(g), and Mo₅O₁₅(g) are from the same source. Cordfunke and Konings⁸ indicate that the overall uncertainties in the enthalpies of formation for these molybdenum trioxide polymers are probably of the order of $\pm 40 \text{ kJ} \cdot \text{mol}^{-1}$ and that these uncertainties are primarily related to uncertainties in the calculated entropies ($\pm 15 \text{ J} \cdot \text{K}^{-1}$ per Mo in each polymer).

Cs₂MoO₄(g)

For Cs₂MoO₄(g), the Cordfunke and Konings' values⁸ were modified based on a later publication from the Petten group.¹¹

CsH(g), Cs₂O(c), Cs₂O(g), and CsO(g)

Values for CsH(g) are derived from the assessment of Glushko et al.,¹² where an uncertainty of $\pm 4 \text{ kJ} \cdot \text{mol}^{-1}$ is suggested for $\Delta_f H^\circ[\text{CsH}(g), 0 \text{ K}]$. Values for Cs₂O(c), Cs₂O(g), and CsO(g) are from the same source.

Cs₂O₂(c) and Cs₂O₂(g)

For Cs₂O₂(c), CHMWRK uses values from Glushko et al.¹² The values for Cs₂O₂(c) have been briefly discussed by Cordfunke and Konings.⁸ That work and an earlier review by Lamoreaux and Hildenbrand¹³ disagree as to the meaning of the results from a relevant experimental study,¹⁴ and the estimates of $\Delta_f H^\circ[\text{Cs}_2\text{O}_2(c), 298.15 \text{ K}]$ differ by $> 100 \text{ kJ} \cdot \text{mol}^{-1}$. The value given in Glushko et al.¹² [$-(440 \pm 25) \text{ kJ} \cdot \text{mol}^{-1}$] is almost equal to the average of the other two and also may be based on an incorrect assumption regarding the nature of the stable solids in the Cs-O system. The values proposed for the entropies and temperature functions^{12,15} appear to be estimates. The CHMWRK values may overestimate the stability of Cs₂O₂(c) with respect to other species. Great caution should be exercised in using the result of any calculation that suggests Cs₂O₂(c) is formed as a major species. For Cs₂O₂(g), CHMWRK uses the values $S^\circ[\text{Cs}_2\text{O}_2(g), 298.15 \text{ K}, 1 \text{ atm}] = 340.8 \text{ J} \cdot \text{K}^{-1} \cdot \text{mol}^{-1}$ (corrected to 1 bar) and $\Delta_f H^\circ[\text{Cs}_2\text{O}_2(g),$

TABLE I

Species from the CHMWRK Database and Thermodynamic Quantities (1 bar) Used in the Chemical Equilibrium Calculations*

Chemical Species	$\Delta_f G^\circ(298.15 \text{ K})$ (kJ·mol ⁻¹)	$S^\circ(298.15 \text{ K})$ (J·K ⁻¹ ·mol ⁻¹)	$\Delta_f G^\circ(1000 \text{ K})$ (kJ·mol ⁻¹)	Reference	Chemical Species	$\Delta_f G^\circ(298.15 \text{ K})$ (kJ·mol ⁻¹)	$S^\circ(298.15 \text{ K})$ (J·K ⁻¹ ·mol ⁻¹)	$\Delta_f G^\circ(1000 \text{ K})$ (kJ·mol ⁻¹)	Reference
O(g)	231.74	161.06	107.8	7,8,9	TeO(OH) ₂	-383.80	332.59	-666.2	7
O ₂ (g)	0.00	205.15	-159.7	7,8,9	TeI ₂ (g)	35.44	345.67	-236.4	7,22
H(g)	203.28	114.71	112.2	7,8,9	TeO ₂ (g)	-68.84	373.40	370.8	7,22
H ₂ (g)	0.00	130.68	-106.6	7,8,9	Cs ₂ Te(c)	-351.80	185.10	-523.8	7,23
OH(g)	34.62	183.74	-109.4	7,8,9	Cs ₂ Te(g)	-118	359.4	-399.2	23
H ₂ O(g)	-228.58	188.84	-379.0	7,8,9	Cs ₂ TeO ₃ (c)	-905.70	232.00	-1144.2	7
I(g)	70.17	180.79	-67.3	7,8,9	Cs ₂ TeO ₄ (c)	-1001.10	233.00	-1254.7	7
I ₂ (g)	19.32	260.69	-182.6	7,8,9	Cs ₂ Te ₂ O ₅ (c)	-1210.60	302.00	-1540 ^a	7
IO(g)	102.47	239.64	-83.88	14	Cs ₂ Te ₄ O ₉ (c)	-1782.70	442.00	-2279 ^a	7
HI(g)	1.70	206.59	-158.5	7,8,9	Mo(c)	0.0	28.56	-33.0	7
HOI(g)	-56.02	254.79	-236.66	16,17	Mo(g)	611.87	181.95	473.6	7
Cs(c)	0.00	85.23	-80.6	7,8,9	Mo ₂ (g)	857.63	244.19	667.9	7
Cs(g)	49.56	175.60	-84.3	7,8,9	MoO(g)	323.22	244.76	133.1	7
Cs ₂ (g)	75.35	284.68	-144.1	7	MoO ₂ (s)	-533.67	46.46	-600.0	7
CsO(g)	19.48	248.51	-176.6	11	MoO ₃ (g)	-76.99	273.91	-743.7	7
Cs ₂ O(g)	-158.09	324.13	-414.2	11	MoO ₃ (c)	-667.92	77.76	-766.6	7
CsOH(c)	-371.80	104.22	-493.68	18	MoO ₃ (g)	-346.58	276.51	-575.7	7
CsOH(g)	-256.51	254.84	-461.77	18	Mo ₂ O ₆ (g)	-1040.40	405.60	-1402.0	7
(CsOH) ₂ (g)	-615.72	381.27	-940.51	18	Mo ₂ O ₉ (g)	-1722.10	549.70	-2228.9	7
CsI(c)	-342.08	123.00	-459.5	7	Mo ₄ O ₁₂ (g)	-2362.10	671.21	-2997.9	7
CsI(g)	-193.65	275.28	-406.0	7	Mo ₅ O ₁₅ (g)	-2982.77	788.50	-3745.6	7
Cs ₂ I ₂ (g)	-507.47	431.40	-852.4	7	H ₂ MoO ₄ (g)	-786.44	355.35	-1096.8	7
CsH(g)	96.69	215.18	-71.7	11	C ₂ MoO ₄ (c)	1406.88	248.35	1667.8	7
Cs ₂ O(c)	-308.79	146.90	-459.9	11	Cs ₂ MoO ₄ (g)	-1149.64	419.056	-1513.9	10
Cs ₂ O ₂ (c)	-381.68	180.00	-563.5	11	UO(g)	14.92	248.97	-178.6	7,24,25
Cs ₂ O ₂ (g)	-236.75	340.95	-515.4	11	UO ₂ (g)	-1145.74	96.11	-1123.8	7,24,25
Te(c)	0.0	49.221	-55.2	7	UO ₃ (g)	-1032.25	83.530	-689.6	7,24,25
Te(g)	169.65	182.71	30.8	7	Cs ₂ UO ₄ (s)	-1805.57	219.66	-2043.5	7
Te ₂ (g)	115.33	258.93	-86.2	7	Cs ₂ U ₂ O ₇ (s)	-3019.08	327.75	-3790 ^a	7
H ₂ Te(g)	85.22	228.46	-95.2	7	Cs ₂ U ₄ O ₁₂ (s)	-5253.57	526.43	-5841.7	7
TeO ₂ (c)	-266.00	69.88	-350.4	7	UO ₂ (ss) ^b	-1032.25	83.53	-1123.2	27
TeO ₂ (g)	-60.32	272.90	-277.5	7	U ₂ O _{4,5} (ss) ^b	-2138.55	164.85	-2322.9	27
TeO(g)	67.03	235.53	-118.4	7	U ₃ O ₇ (ss) ^b	-3234.37	290.17	-3542.9	27
Te ₂ O ₂ (g)	-80.77	327.30	-349.1	4					

*Values of $\Delta_f G^\circ$ at 1000 K are with respect to the elements at 298.15 K. Values of the thermodynamic quantities have not been rounded to reflect their uncertainties.

^aPrimary data used for this species are not suitable for calculations for 1000 K.

^bValues are for use with the solid solution model of Lindemer and Besmann²⁸ and are not values for the pure solids.

298.15 K] = -247.084 kJ·mol⁻¹ from Glushko et al.¹² in which the uncertainty in $\Delta_f H^\circ[\text{Cs}_2\text{O}_2(\text{g}), 0 \text{ K}]$ is estimated as $\pm 20 \text{ kJ}\cdot\text{mol}^{-1}$. There appears to be an error in the sign in the Cordfunke and Konings' value [(251 \pm 25) kJ·mol⁻¹] for $\Delta_f H^\circ[\text{Cs}_2\text{O}_2(\text{g}), 298.15 \text{ K}]$ (Ref. 8).

IO(g)

Values for iodine oxides were recently reevaluated by Chase.¹⁵ From the values given in Ref. 15, thermodynamic parameters for IO(g) were incorporated into the database, and $\Phi(T)$ coefficients were selected. The selected value of the enthalpy of formation at 298.15 K, (126 \pm 18) kJ·mol⁻¹, is larger than the more recent value, (115.9 \pm 5.0) kJ·mol⁻¹, proposed by Bedjanian et al.¹⁶ However, the values agree within the stated uncertainties.

HOI(g)

The thermodynamic quantities for HOI(g) have been in dispute for many years.^{8,17} Selected values were generally based on estimated values for the bond energies or the Gibbs energy of vaporization. Recent work by Zhang et al.¹⁸ has shed new light on this problem. In their work, $\Delta_f H^\circ[\text{HOI}(\text{g}), 0 \text{ K}] = -(42.7 \pm 2.5) \text{ kJ}\cdot\text{mol}^{-1}$ was estimated based on new spectroscopic and kinetic studies of IO(g), and examination of bonding trends for OX and HOX species (X = Cl, Br, I).¹⁸ From that value and $S^\circ[\text{HOI}(\text{g}), 298.15 \text{ K}, 1 \text{ bar}] = 254.67 \text{ J}\cdot\text{K}^{-1}\cdot\text{mol}^{-1}$ estimated by Garisto,¹⁷ $\Delta_f H^\circ[\text{HOI}(\text{g}), 298.15 \text{ K}] = -47.43_3 \text{ kJ}\cdot\text{mol}^{-1}$. This indicates that HOI(g) is 30 to 40 kJ·mol⁻¹ less stable at 298.15 K than previous estimates,^{8,17} which means that HOI(g) is only a very minor species [compared

to $I_2(g)$] for systems containing liquid water near, or slightly above, room temperature. Values of the coefficients for $\Phi(HOI(g), T)$ were calculated from the $\Phi(T)$ values tabulated by Garisto.¹⁷

CsOH(c), CsOH(g), and (CsOH)₂(g)

The $\Phi(T)$ coefficients for solid and liquid forms of CsOH were calculated from the heat capacity equations of Gurvich et al.¹⁹ The heat capacity equation for CsOH(cr, β) was given twice in Ref. 19, and there are typographical errors in both versions. The following equation, consistent with the values tabulated in Ref. 19, was used:

$$\begin{aligned} C_p^o(\text{CsOH}, \beta, T) / J \cdot K^{-1} \cdot \text{mol}^{-1} \\ = -46.557 + 395.682 \times 10^{-3} T \\ + 24.848 \times 10^5 T^{-2} - 331.165 \times 10^{-6} T^2 \end{aligned}$$

The $\Phi(T)$ coefficients for CsOH(g) and (CsOH)₂(g) were determined by fitting the values of $\Phi(T)$ tabulated by Gurvich et al.¹⁹ In each case, the values from 298.15 to 1500 K and 1500 to 6000 K were fitted separately to provide better values over the entire temperature range. The lower-temperature fits were constrained so that $S^o(298.15 \text{ K})$ is exactly equal to $\Phi(298.15 \text{ K})$.

Te(s), Te(g), Te₂(g), H₂Te(g), TeO₂(c), and TeO(OH)₂(g); Cs₂TeO₃(c), Cs₂TeO₄(c), Cs₂Te₂O₅(c), Cs₂Te₄O₉(c), and Cs₂Te₄O₁₂(c)

The values for Te(s), Te(g), Te₂(g), H₂Te(g), TeO₂(g), and TeO(OH)₂(g) in the CHMWRK database are derived from the tables of Cordfunke and Konings.⁸ Values for the ternary cesium tellurates also come from the same source.⁸

TeO(g) and TeO₂(g)

The CHMWRK values for TeO(g) and TeO₂(g) are from Cordfunke and Konings.⁸ For reasons discussed by Cordfunke and Konings,⁸ Pankratz's²⁰ value for $\Delta_f H^o[\text{TeO}_2(g)]$ is more negative than that selected for CHMWRK. The enthalpy of formation of TeO(g) depends on the value for TeO₂(g).

Te₂O₂(g)

There are no values for Te₂O₂(g) in Cordfunke and Konings⁸ or in any of the volumes of Glushko et al.¹² For CHMWRK, Garisto⁴ used the values from Mills²¹ (based on the experimental work of Muenow et al.²²) but updated them using the Cordfunke and Konings⁸ values for TeO(g) and data for the monomer-dimer equilibrium constant.²¹

TeI₂(g) and TeOI₂(g)

The values for the complicated Te-I and Te-I-O systems in the CHMWRK database are incomplete and are based on experimental work that needs further confirmation. The value for $\Delta_f H^o[\text{TeIO}_2(g)]$ was calculated from the reanalysis of the experimental data of Oppermann et al.²³ The values of $\Phi(T)$ to 2000 K come from Cordfunke and Konings⁸; S^o and $\Phi(T)$ for TeI₂(g) are from Cordfunke and Konings,⁸ and the value for $\Delta_f H^o[\text{TeI}_2(g)]$ comes from the reanalysis of Oppermann et al.²³

Cs₂Te(c), Cs₂Te(g), and Cs₂Te₃(c)

The values for these three species are from McFarlane.²⁴ The values for temperatures < 1000 K for Cs₂Te(c) are those used by Cordfunke and Konings.⁸

UO(g), UO₂(g), and UO₃(g)

The CHMWRK database values are from Cordfunke and Konings,⁸ who relied heavily on the analysis of Fisher.^{25,26}

UO_{2+x}(s)

Garisto²⁷ used the thermodynamic model of Lindemer and Besmann²⁸ to introduce a representation of UO_{2+x} as an ideal solution of UO₂(s) and U₂O_{4,5}(s) for x less than a calculated, experimentally-based limit, and as an ideal solution of UO₂(s) and U₃O₇(s) for greater values of x . The point at which the representation of UO_{2+x} changes from UO₂(s)-U₂O_{4,5}(s) to UO₂(s)-U₃O₇(s) is dependent on the stoichiometry of the solid and the temperature.

CsUO₄(s), Cs₂U₂O₇(s), and Cs₂U₄O₁₂(s)

Cordfunke and Konings⁸ is the source of the thermodynamic data for CsUO₄(s), Cs₂U₂O₇(s), and Cs₂U₄O₁₂(s), the only cesium uranate species that will form in fuel under normal or accident conditions. Another uranate, CsUO_{3.56}(s), can form under very reducing conditions, such as in the presence of liquid cesium, which will not occur in any CANDU accident scenario.

Species Not Included

There is good evidence for the existence of CsO₂(c), but there has been much debate as to the values for its thermodynamic quantities; hence, it is not included in the CHMWRK database. Its inclusion would not be expected to affect the results significantly. There is a brief assessment in the Cordfunke and Konings⁸ review where a value of $-230 \text{ J} \cdot \text{K}^{-1} \cdot \text{mol}^{-1}$ to $-240 \text{ J} \cdot \text{K}^{-1} \cdot \text{mol}^{-1}$ for $\Delta_f H^o[\text{CsO}_2(c), 298.15 \text{ K}]$ is suggested; this is a less negative value than values (near $-286 \text{ kJ} \cdot \text{mol}^{-1}$)

reported by Lamoreaux and Hildenbrand¹³ and Glushko et al.¹²

Cordfunke and Konings⁸ did not suggest values for $\text{CsO}_2(\text{g})$. Rough estimates provided by Garisto⁴ and Lamoreaux and Hildenbrand¹³ do not agree well. No values have been included in CHMWRK.

There are no values for $\text{MoOH}(\text{g})$ and $\text{Mo}(\text{OH})_2(\text{g})$ in the CHMWRK database. Cordfunke and Konings⁸ provide a brief discussion, but values are estimated for only three temperatures (in the range 1000 to 2000 K).

No values for $\text{Cs}_2\text{Mo}_2\text{O}_7(\text{s})$, $\text{Cs}_2\text{Mo}_3\text{O}_{10}(\text{s})$, $\text{Cs}_2\text{Mo}_4\text{O}_{13}(\text{s})$, $\text{Cs}_2\text{Mo}_5\text{O}_{16}(\text{s})$, and $\text{Cs}_2\text{Mo}_7\text{O}_{22}(\text{s})$ (Ref. 29) are included in the CHMWRK database. The regions of stabilities for these solids are likely to be small, but further information would be useful. For similar reasons, the species $\text{MoI}(\text{s})$, $\text{MoI}(\text{g})$, $\text{MoI}_2(\text{s})$, $\text{MoI}_2(\text{g})$, $\text{MoI}_3(\text{s})$, $\text{MoI}_3(\text{g})$, $\text{MoI}_4(\text{s})$, $\text{MoI}_4(\text{g})$, and $\text{MoO}_2\text{I}_2(\text{g})$ have not been included in the CHMWRK database.

There is evidence for the existence of $\text{Te}_2\text{O}_4(\text{g})$, but neither Mills²¹ nor Cordfunke and Konings⁸ recommend temperature functions for this species. At present, no database values can be recommended for $\text{Te}_2\text{O}_4(\text{g})$, although recent work by Narasimhan et al.³⁰ may be useful in any assessment. $\text{Cs}_2\text{Te}_4\text{O}_{12}(\text{s})$ and $\text{Cs}_2\text{TeO}_3(\text{g})$ probably exist³¹ but are not included in the database.

II.B. Comparison of Thermodynamic Calculations with Experimental Data

The CHMWRK code/database predictions for cesium-iodine-molybdenum-urania systems were compared to experimental results obtained by Knudsen-cell mass spectrometry.

II.B.1. Knudsen-Cell Experiments

As the Knudsen-cell experiment is described in detail in an earlier publication,⁵ only a brief synopsis is presented here.

Knudsen-cell mass-spectrometric analysis was used to study cesium-iodine-molybdenum-urania systems up to 2700 K. Samples were inductively heated in a tantalum cell, using a Radyne 17-kW power supply. Temperatures were monitored by focusing a dual-wavelength optical pyrometer into a side blackbody cavity drilled into the lower portion of the cell. Ion signals were obtained as a function of temperature using a Finnigan quadrupole mass spectrometer. Ionizing electrons were normally accelerated to 70 eV. Ion signals were converted to vapor pressures using the method of ion ratios, and they relied on a calibration with silver.³² Vapor pressures were estimated to be accurate within a factor of 2. The main source of the uncertainty arose from the ionization cross sections used in the vapor pressure calculations.³³ Appearance potentials were recorded to determine the provenance of the ions observed in the mass spectrometer. Second-law heats of vaporization were also measured.

Samples heated inside the cell included

Cs_2MoO_4

CsI and MoO_2 (1:1 mole ratio)

CsI , Mo , and $\text{UO}_{2.00}$ (1:1.3:4.5 mole ratio)

CsI , Mo , and $\text{UO}_{2.01}$ (1:1.3:4.5 mole ratio)

CsI and $\text{UO}_{2.00}$ (0.04:1 mole ratio).

Vapor pressures of Cs_2MoO_4 above cesium molybdate and various reaction mixtures are presented in Fig. 1. The dashed lines representing experimental results serve only to clarify the presentation. Reactions were observed between CsI and MoO_2 , and between CsI , Mo , and UO_{2+x} to form Cs_2MoO_4 . Particularly in the case of CsI and MoO_2 , sufficient reaction occurred such that product Cs_2MoO_4 was also observed by Fourier transform infrared spectroscopy in the same study.⁵ Iodine, as I_2^+ , was observed for all of the heated mixtures at temperatures < 800 K. However, thermodynamic data could not be derived from the signal; the vapor pressure of iodine changed with time, indicating chemical equilibrium had not been achieved in the Knudsen cell at temperatures < 800 K.

At higher temperatures, the vapor pressure of Cs_2MoO_4 was found to be much more stable, and thus, yields from different chemical systems could be compared. The vapor pressures measured above pure cesium molybdate were within an order of magnitude of the

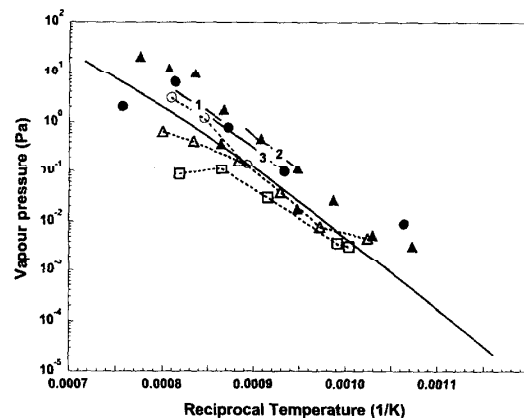


Fig. 1. Plot of partial pressure of Cs_2MoO_4 as a function of reciprocal temperature (K^{-1}). The points and dashed lines refer to experimental results: filled triangles and circles: above Cs_2MoO_4 ; open circles: above CsI/MoO_2 ; open triangles: above $\text{CsI}/\text{Mo}/\text{UO}_{2.01}$; open squares: above $\text{CsI}/\text{Mo}/\text{UO}_{2.00}$. The solid lines represent published data: 1: Tangri et al.⁴²; 2: Yamawaki et al.⁴³; and 3: Cordfunke et al.¹⁰ The CHMWRK simulation is the long unmarked solid line.

literature values, and often closer, especially at high temperatures. The vapor pressure of cesium molybdate above the CsI-molybdenum-urania mixtures was lower than that over the pure $\text{Cs}_2\text{MoO}_4(\text{c})$, suggesting an activity coefficient of ~ 0.1 for Cs_2MoO_4 in the solid. Integrating the curve of ion signal with time allowed a comparison of the extent of reaction for CsI and MoO_2 , CsI, Mo, and $\text{UO}_{2.00}$ and CsI, Mo, and $\text{UO}_{2.01}$. The ratio of the integrated areas was found to be 900:44:55, indicating that the reactivity of CsI and Mo in the presence of UO_{2+x} was quite low.

The conclusions of the Knudsen-cell experiments were that the reaction of CsI with elemental molybdenum is unlikely to be a major contributor to molybdate formation, even in the presence of slightly hyperstoichiometric fuel. However, cesium molybdate is readily

formed at higher oxygen potentials, such as in the presence of MoO_2 , suggesting a role for the ternary compound in an accident involving oxidizing conditions.

H.B.2. Computer Simulation of Partial Pressures of Cs_2MoO_4

Thermodynamic calculations were performed to simulate the results of the Knudsen-cell experiments. The calculations included data for species of the elements: cesium, iodine, molybdenum, uranium, hydrogen, and oxygen, as listed in Table I. Values of input variables are given in Table II, and these correspond directly to experimental conditions. The inputs include the number of moles of the reagents, the volume of the cell (since these were tests that were undertaken under conditions of

TABLE II
Values of Input Variables for CHMWRK Simulation of Knudsen-Cell Experiments*

Chemical System	Amounts (mol)	Temperature (K)	Notes
$\text{Cs}_2\text{MoO}_4(\text{s})$	1.5×10^{-3}	400 to 1500	Simulates heating of pure Cs_2MoO_4 [86C1,86D2 (Ref. 5)]
CsI(s)	1.5×10^{-3}	400 to 1500	Cs/Mo = 1:1 [87A2 (Ref. 5)]
$\text{MoO}_2(\text{s})$	1.5×10^{-3}		
CsI(s)	3.0×10^{-3}	400 to 1500	Cs/Mo = 2:1
$\text{MoO}_2(\text{s})$	1.5×10^{-3}		
CsI(s)	1.5×10^{-3}	400 to 1500	Cs/Mo = 1:2
$\text{MoO}_2(\text{s})$	3.0×10^{-3}		
CsI(c)	1.5×10^{-3}	400 to 1500	$\text{UO}_{2.000}$ [87D1,87E1 (Ref. 5)]
Mo(s)	1.5×10^{-3}		
UO(g)	3.75×10^{-3}		
$\text{UO}_3(\text{g})$	3.75×10^{-3}		
CsI(c)	1.5×10^{-3}	400 to 1500	$\text{UO}_{2.010}$
Mo(s)	1.5×10^{-3}		
UO(g)	3.7125×10^{-3}		
$\text{UO}_3(\text{g})$	3.7875×10^{-3}		
CsI(c)	1.5×10^{-3}	400 to 1500	$\text{UO}_{2.001}$
Mo(s)	1.5×10^{-3}		
UO(g)	3.74625×10^{-3}		
$\text{UO}_3(\text{g})$	3.75375×10^{-3}		
CsI(c)	1.5×10^{-3}	400 to 1500	$\text{UO}_{2.100}$
Mo(s)	1.5×10^{-3}		
UO(g)	3.375×10^{-3}		
$\text{UO}_3(\text{g})$	4.125×10^{-3}		
CsI(c)	3.0×10^{-4}	400 to 1500	$\text{UO}_{2.000}$ [82K (Ref. 33)]
UO(g)	3.75×10^{-3}		
$\text{UO}_3(\text{g})$	3.75×10^{-3}		
CsI(c)	1.5×10^{-3}	400 to 1500	$\text{UO}_{2.000}$
UO(g)	3.75×10^{-3}		
$\text{UO}_3(\text{g})$	3.75×10^{-3}		

*The constant volume used in all calculations simulating Knudsen-cell experiments was $2.5 \times 10^{-3} \text{ dm}^3$.

constant volume), and the temperatures over which the samples were heated. Additional runs were performed to assess system response to a greater range of conditions than was explored in the experiments. For instance, the cesium-to-molybdenum ratio was varied from 2:1 to 1:2, even though experiments were done with a 1:1 ratio. The stoichiometry of the UO_{2+x} was varied from $\text{UO}_{2.000}$ to $\text{UO}_{2.100}$.

The results of the calculations are presented in Fig. 1 (long solid line), together with the experimental data, and are summarized in Table III. The calculated partial pressures of Cs_2MoO_4 above pure $\text{Cs}_2\text{MoO}_4(\text{c})$ and above the reactive mixtures were the same above 800 K and are shown as one line on the graph. The computational results coincided with the experimental points for the $\text{CsI} + \text{MoO}_2$ mixture. For pure Cs_2MoO_4 , the calculated $RT \ln[p(\text{O}_2)/\text{bar}]$ ranged from $-254.11 \text{ kJ}\cdot\text{mol}^{-1}$ at 400 K to $-194.94 \text{ kJ}\cdot\text{mol}^{-1}$ at 1500 K.

In the case of $\text{CsI} + \text{MoO}_2$, formation of $\text{Cs}_2\text{MoO}_4(\text{c})$ was predicted in the condensed phase, but the extent of reaction was $<10^{-9}$ at 1000 K and only 10^{-5} at 1500 K. The partial pressure of oxygen was much lower for the mixture than for pure cesium molybdate; $RT \ln[p(\text{O}_2)/\text{bar}]$ ranged from $-304 \text{ kJ}\cdot\text{mol}^{-1}$ at 400 K, through a minimum of $-460 \text{ kJ}\cdot\text{mol}^{-1}$ at 700 K, to $-323 \text{ kJ}\cdot\text{mol}^{-1}$ at 1500 K. The oxygen potential of the mixture was the same as that above MoO_2 at temperatures $>1000 \text{ K}$. The gas phase was dominated by $\text{CsI}(\text{g})$ and $\text{Cs}_2\text{I}_2(\text{g})$. The reaction product $\text{I}_2(\text{g})$ was present at a partial pressure several orders of magnitude lower than that of $\text{Cs}_2\text{MoO}_4(\text{g})$, ranging from $2 \times 10^{-19} \text{ Pa}$ (negligible vol-

atility) at 600 K to 0.02 Pa at 1500 K. Changes in the cesium-to-molybdenum ratio, from 2:1 to 1:2, had no effect on the results of the calculation for the $\text{CsI}-\text{MoO}_2$ system.

In some experiments, I_2 was observed at low temperatures, from 479 to 800 K. The pressures of I_2 ranged from 10^{-3} to 5 Pa, but the corresponding Clausius-Clapeyron plots were not linear, suggesting that the chemical system was not at equilibrium. The measured pressures were higher than those calculated for chemical equilibrium conditions.

Under experimental conditions, the $\text{CsI}(\text{g})$ pressure became sufficiently large at temperatures above 1000 K to violate the principles of effusion from the orifice and minimal perturbation of the chemical equilibrium in the Knudsen cell.³³ In practice, the heating was not continued beyond 1000 K until the CsI was completely volatilized, driving the solid-state reaction to produce $\text{Cs}_2\text{MoO}_4(\text{s})$. The ion signal from $\text{Cs}_2\text{MoO}_4(\text{g})$ was observed as the temperatures were further increased from 1000 to $>1400 \text{ K}$.

Calculations were performed for the system $\text{CsI} + \text{Mo} + \text{UO}_{2+x}$. When the stoichiometry of the urania was $\text{UO}_{2.000}$, no formation of $\text{Cs}_2\text{MoO}_4(\text{s} \text{ or } \text{g})$ was predicted, and the main gas-phase species was $\text{CsI}(\text{g})$. For slightly hyperstoichiometric urania, formation of $\text{MoO}_2(\text{s})$ and $\text{Cs}_2\text{MoO}_4(\text{s}, \text{g})$ did occur, mainly the former. The partial pressures of $\text{Cs}_2\text{MoO}_4(\text{g})$ in equilibrium with $\text{CsI} + \text{Mo} + \text{UO}_{2+x}$ were the same as those calculated for equilibrium with $\text{CsI} + \text{MoO}_2$, and with pure Cs_2MoO_4 , for temperatures above 800 K. The partial

TABLE III
Summary of Calculated and Experimental Knudsen Cell Results*

	Temperature (K)	Cs_2MoO_4	$\text{CsI} + \text{MoO}_2$	$\text{CsI} + \text{Mo} + \text{UO}_{2.000}$	$\text{CsI} + \text{Mo} + \text{UO}_{2.0001}$	$\text{CsI} + \text{Mo} + \text{UO}_{2.010}$
Pressure I_2 (Pa)	700	Not part of system	4.0×10^{-17} (3.9)	3.0×10^{-17} (0.082)	7.3×10^{-17}	9.7×10^{-17} (0.094)
Pressure Cs_2MoO_4 (Pa)	700	3.4×10^{-10}	3.4×10^{-10}	No Cs_2MoO_4 observed or calculated	1.9×10^{-10}	1.4×10^{-10}
	1000	9.2×10^{-4} (0.0033)	9.2×10^{-4} (0.0099)	No Cs_2MoO_4 calculated (0.0016)	9.2×10^{-4}	9.1×10^{-4} (0.0024)
	1300	1.2 (5.5)	1.2 (2.4)	No Cs_2MoO_4 calculated (0.16)	1.2	1.2 (0.54)
Oxygen potential ($\text{kJ}\cdot\text{mol}^{-1}$)	700	-255	-460	-1527	-460	-460
	1000	-246	-407	-1256	-407	-407
	1300	-214	-356	-1154	-356	-356

*The experimental Knudsen-cell results are in parentheses. If experimental results are not given in the table, the species were not observed for the given chemical system at the given temperature. The detection limit in the Knudsen-cell apparatus is $\sim 10^{-3} \text{ Pa}$ for most species.

pressures of $\text{Cs}_2\text{MoO}_4(\text{g})$ were lower for the urania system below 800 K because little cesium molybdate was formed. Similarly, there was agreement in the calculated amount of $\text{I}_2(\text{g})$ formed at 800 K and above, for $\text{CsI} + \text{MoO}_2$, and $\text{CsI} + \text{Mo} + \text{UO}_{2+x}$ ($x > 0$). The oxygen potential of the system also mimicked that of $\text{CsI} + \text{MoO}_2$ above 700 K for all three systems of UO_{2+x} ($x = 2.001, 2.010, \text{ and } 2.100$).

Thermodynamic calculations were also performed for the system $\text{CsI} + \text{UO}_{2.000}$, without the presence of molybdenum. These calculations showed that the chemical system was essentially nonreactive and that the main gas-phase species were from the volatilization of CsI . The partial pressure of CsI was the same as observed for the other chemical systems heated in the Knudsen cell and modeled using the CHMWRK code.

The results of the CHMWRK analysis and the Knudsen-cell experimental data agreed to within an order of magnitude up to 1200 K, and between 770 and 1150 K, the agreement was within a factor of 2 to 5 depending on the chemical system, except for the $\text{CsI} + \text{Mo} + \text{UO}_{2.00}$ system where some Cs_2MoO_4 product was observed in the Knudsen cell but none was predicted by calculation. The discrepancy could be attributed to the difficulty in obtaining $\text{UO}_{2.00}$ and measuring the stoichiometry of the uranium oxide solid. Even slight surface oxidation could lead to a reaction to produce Cs_2MoO_4 . For the other systems, the agreement between experiment and calculation was satisfactory given the uncertainties in calculating absolute vapor pressure in the Knudsen cell and hence provided confidence that CHMWRK could be used to model chemical systems of cesium-iodine-molybdenum and slightly hyperstoichiometric urania that are in thermodynamic equilibrium.

The code did not reproduce the reactions occurring at relatively low temperatures (< 800 K) in the Knudsen cell and the partial pressure of I_2 that was observed experimentally. The discrepancy between calculation and experiment likely arose because the composition of the chemical system was controlled by kinetics at temperatures < 800 K. In addition, the CHMWRK calculation did not automatically allow for the depletion of CsI from the Knudsen cell, as observed in the experiments. To properly model this effect, separate code simulations would have to be performed, with prior knowledge of the time-dependent composition of the condensed phase remaining in the cell. Such data would have been difficult to obtain from the Knudsen-cell experiments.

II.C. Conditions for Calculation of Iodine Speciation in a Reactor Accident

The envelope of conditions established for the thermodynamic calculations was defined to approximate those representative of conditions following a LOCA with loss-of-emergency core cooling (LOCA-LOECC) addressed in CANDU safety analyses. The objective of the

TABLE IV
Mass Concentrations of Fission Products in HTS
(CANDU Fuel)*

Fission Product	Inventory ³⁹ (g/kg U) (from ORIGEN calculations, 190 MWh/kg U burnup)	Mass Concentration ($\text{g} \cdot \text{m}^{-3}$ steam)
Iodine	0.062	0.33
Tellurium	0.11	0.67
Cesium	0.62	2.9
Molybdenum	0.70	1×10^{-5} (assuming release rate to be the same as that of uranium—neutral or reducing conditions)

*The source is Ref. 35.

study was to predict the volatile mole fraction of iodine in the channel for prescribed temperature/pressure conditions prior to release to containment. The elements included in the HTS chemical thermodynamic calculations were iodine, cesium, hydrogen, oxygen, tellurium, molybdenum, and uranium, and the species listed in Table I.

Physical properties such as pressure and total number of gaseous moles were chosen to give a reaction volume equivalent to the flow space in a CANDU fuel channel, $\sim 20 \text{ dm}^3$. These calculations were performed assuming that the channel was dry and that the coolant flow was either pure $\text{H}_2\text{O}(\text{g})$, pure $\text{H}_2(\text{g})$, or a gaseous mixture of $\text{H}_2\text{O}/\text{H}_2$.

Concentrations of fission product iodine and cesium in steam under standard conditions (see Sec. III.A) were based on CORSOR^e correlations for fuel releases (Table IV). The steam temperature profile in the channel, used for these estimates, ranged from a maximum of 2400 K in the vicinity of the failed fuel to a minimum value of 900 K at the upstream end of the channel. The fission product concentrations in Table IV represent estimates of the maxima expected in a steam environment for a LOCA-LOECC accident scenario. The predicted fission product concentrations will be much lower at the beginning and end of the transient, or when the out-bound flow from channels with failed fuel and those without failed fuel are mixed together, or in less severe accidents.

In addition to the speciation under the reference conditions described above, iodine speciation was examined

^eCORSOR uses empirical correlations to calculate fission product release rates, assuming that these are first-order processes. The output of the CORSOR code is in the form of Arrhenius plots of fractional release rate.³⁴

as a function of a number of different parameters because of the wide range of thermodynamic conditions for various accident scenarios and because of uncertainties in elemental abundance. These sensitivity studies were performed to determine the effects of the following on iodine speciation in the HTS, or on the initial iodine speciation released to containment:

1. changes in cesium-to-iodine ratio
2. changes in iodine concentration in the coolant
3. changes in oxygen partial pressure.

The calculations reported in this paper extend earlier calculations, which focused on the effect of the cesium-to-iodine ratio on iodine speciation.⁴

Processes such as condensation onto aerosols, transport in the channel, or reaction with the pressure tube were not considered in these calculations. Some of these effects have the potential to reduce the cesium-to-iodine ratio, such as the gas-phase reaction of cesium with tin to form Cs_2SnO_3 or heterogeneous reaction with aerosols. Other effects, such as iodine retention or reaction with system materials, would mitigate the release of volatile iodine. The sensitivity study performed here should help test the predictions by comparing them with overestimation and underestimation of the amount of volatile iodine formed in the channel.

III. RESULTS AND DISCUSSION

Iodine speciation predictions using CHMWRK are shown in Fig. 2 (standard conditions as defined below), Fig. 3 (a reduced cesium to iodine ratio in steam), Fig. 4 (a reduced iodine to steam ratio in steam), Fig. 5 (iodine speciation in 50% $H_2O/50\% H_2$), and Fig. 6 (a reduced cesium to iodine ratio in 50% $H_2O/50\% H_2$). The volatile iodine species, which include I_2 , HI, and HOI, are of particular interest in safety analysis as they would be gaseous under the low-temperature containment conditions, and hence are more mobile than the CsI or Cs_2I_2 . All of these compounds are shown in Figs. 2 through 6 if they comprised more than 10^{-4} mole fraction of the initial iodine, as predicted from the calculations.

III.A. Standard Conditions

The calculations were referenced to a set of standard conditions, derived in the context of a LOCA-LOECC event as discussed in Sec. II.C. The standard conditions for the purposes of this report were

1. a cesium-to-iodine mole ratio of 10
2. an iodine-to-steam mole ratio of 2.5×10^{-5}
3. a constant steam pressure of 1.2 MPa.

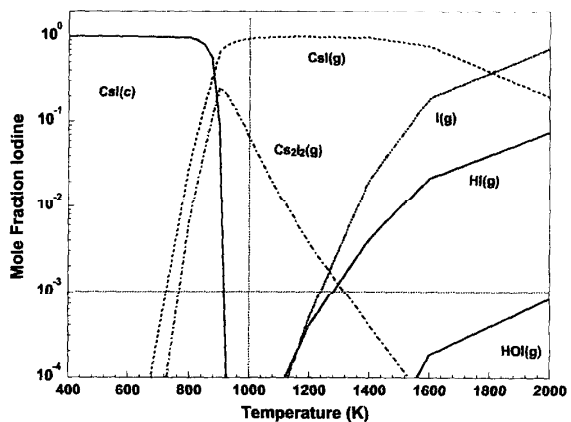


Fig. 2. Mole fraction of iodine as a function of temperature (K). Thermodynamic equilibrium calculations were performed assuming standard conditions (a cesium-to-iodine ratio of 10 and an iodine-to-steam mole ratio of 2.5×10^{-5}). The pressure of the steam was 1.2 MPa. Condensed phase is designated as (c). Other species are in the gas phase. The lines indicate the safety analysis reference conditions of 10^{-3} mole fraction (0.1%) iodine and 1000 K.

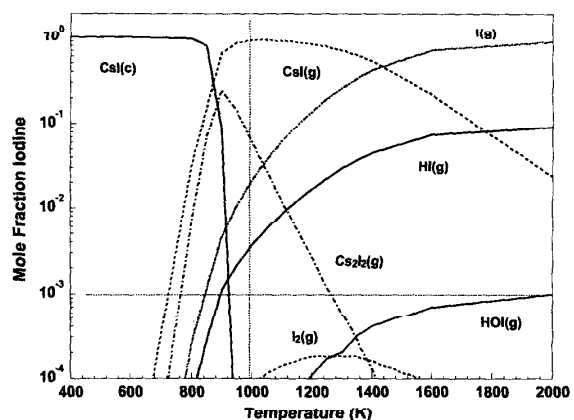


Fig. 3. Mole fraction of iodine as a function of temperature (K). Thermodynamic equilibrium calculations were performed assuming a reduced cesium-to-iodine ratio in otherwise standard conditions (an iodine-to-steam mole ratio of 2.5×10^{-5} and a pressure of 1.2 MPa). The cesium-to-iodine ratio was assumed to be 1. Condensed phase is designated as (c). Other species are in the gas phase.

Fission product and steam ratios were based on estimation of concentrations in the HTS as shown in Table IV. The thermodynamic equilibrium calculations for the standard case with a Cs/I ratio of 10 (Fig. 2) show that

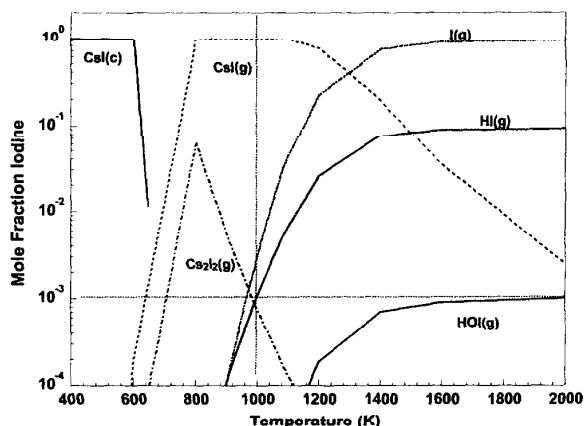


Fig. 4. Mole fraction of iodine as a function of temperature (K). Thermodynamic equilibrium calculations were performed assuming a reduced iodine to steam ratio in otherwise standard conditions (a cesium-to-iodine ratio of 10). The amount of iodine release was taken as 10⁻⁶ mole into 4 mol of steam (giving a mole ratio of 2.5 × 10⁻⁷) at 1.2 MPa. Condensed phase is designated as (c). Other species are in the gas phase. The dashed line indicates the rapid drop in condensed phase CsI from 600 K down to a negligible amount (off scale) at 800 K.

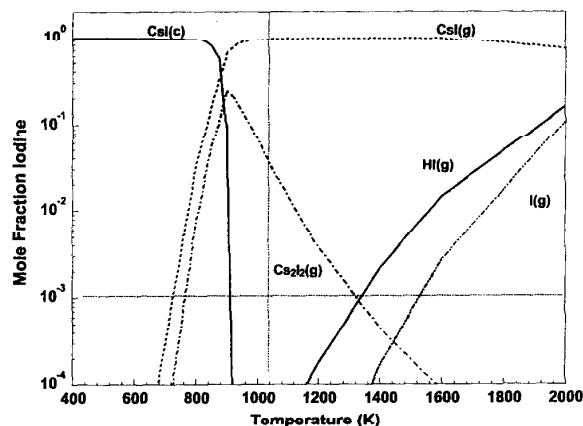


Fig. 5. Mole fraction of iodine as a function of temperature (K). Thermodynamic equilibrium calculations were performed assuming the release of 0.0001 mole iodine into 2 mol steam and 2 mol H₂ at 1.2 MPa. The cesium-to-iodine ratio was assumed to be 10. Condensed phase is designated as (c). Other species are in the gas phase. The fractions of HI and I at 1000 K are well below 10⁻⁴, outside the y-axis range.

volatile iodine percentage would be significantly less than 0.1% at 1000 K (Ref. 4), using CANDU reactor safety analysis reference conditions. At higher temperatures, the major gaseous iodine species are CsI, HI, and I. A small amount of HOI is formed above 1600 K. The fraction of iodine as I₂ never exceeded 10⁻⁵ and so is not shown in Fig. 2. The thermodynamic stability of CO and CO₂ and the radiolytic decomposition of organic compounds make organic iodide formation in the HTS unlikely. Organic iodide formation was considered in previous calculations and was found to be negligible.⁴

III.B. Dependence on Cesium-to-Iodine Mole Ratio

Although the chemical thermodynamic database contains the most important chemical compounds for reactor safety analysis, data for some species are missing such as the cesium stannates^{36,37} and cesium rare-earth oxides.³⁸ A sensitivity analysis of the cesium-to-iodine ratio was performed to compensate for missing species.

When the initial cesium concentration is reduced by a factor of 10, giving a cesium-to-iodine ratio of 1, the gaseous fraction at 1000 K is increased to 2% (Fig. 3). In the fuel, the cesium-to-iodine ratio is expected to be ~9. However, the cesium-to-iodine ratio could be lowered if the cesium is tied up as molybdates, tied up as uranates, or combines with the tin in Zircaloy as Cs₂SnO₃. The combination with other elements, for which the reaction

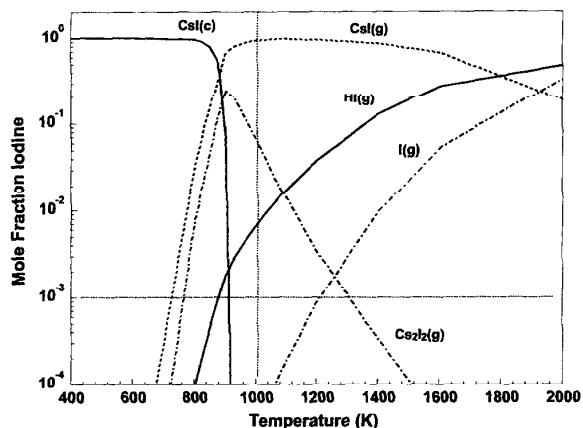


Fig. 6. Mole fraction of iodine as a function of temperature (K). Thermodynamic equilibrium calculations were performed assuming a reduced cesium-to-iodine ratio in 2 mol steam and 2 mol H₂ at 1.2 MPa. The cesium-to-iodine ratio was assumed to be 1, and the amount of iodine in the steam was taken as 0.0001 mol. Condensed phase is designated as (c). Other species are in the gas phase.

with molybdenum gives the most concern, is discussed in Sec. III.F.

III.C. Dependence on Iodine Concentration in Steam

The post-blowdown steam discharge during a LOCA-LOECC scenario can continue for hundreds of seconds.

During this time, the steam flow is gradually decreasing. As discussed in Sec. I, the rate of release of fission products is related to the steam flow, being balanced by cooling on one hand and on feeding of the zirconium-water reaction on the other. The worst conditions for fission product release are at low flows of 5 to 10 $\text{g}\cdot\text{s}^{-1}$. The concentration of iodine will be reduced at high steam flow rates. Hence, calculations were performed to investigate the sensitivity of the iodine speciation to iodine concentration. An example is shown in Fig. 4, where the amounts of iodine and cesium were reduced by two orders of magnitude from the standard condition with a cesium-to-iodine ratio of 10.

At the reference temperature of 1000 K, the mole fraction of volatile iodine [as $\text{I}(\text{g})$ and $\text{HI}(\text{g})$] is now 0.004 under conditions of reduced concentration. Although the mole fraction of volatile iodine increases as the overall concentration in steam decreases, the absolute number of moles of iodine released under these conditions is small, and so is the source term to containment, e.g., 1% of 0.4% = 0.004% of the total iodine inventory that would be released in volatile form in the scenario. Low iodine concentration conditions may occur at the beginning and the end of fission product release or under conditions of prefailed fuel.

III.D. Dependence on Oxygen Potential of the Coolant

The speciation of the fission products also depends on the H/O ratio (oxygen partial pressure). Reducing steam conditions ($\text{H}/\text{O} > 2$) are expected in the HTS at higher temperatures (>1700 K) because of production of hydrogen by the zirconium-water reaction. When half of the steam is converted to hydrogen, the fraction of HI increases, but the fraction of I decreases. For the steam/ H_2 condition with a Cs/I ratio of 10, the mole fraction of volatile iodine (i.e., the sum of HI and I fractions) at 1000 K is very small, $<10^{-5}$ (Fig. 5).

The mole fraction of iodine species other than CsI or Cs_2I_2 at 1000 K could reach 0.7% when the Cs/I ratio is reduced to 1 in 50% steam–50% H_2 (Fig. 6). However, the major component of this “volatile” iodine is HI, which is very water soluble and thus is expected to dissolve quickly into condensing steam when discharged into containment.

III.E. Dependence on System Pressure

The total system pressure in accident scenarios varies greatly, from 10 to 12 MPa (normal CANDU system pressure) in single-channel accident scenarios, to 0.2 to 0.5 MPa (near-ambient pressure) near the end of a LOCA-LOECC scenario. Most of the calculations discussed in Secs. III.A through III.D were performed for an intermediate pressure of 1.2 MPa. The oxygen potential of steam and hydrogen-steam mixtures would be expected to increase somewhat with pressure, in accordance with

Le Chatelier's principle. The scope of these calculations was extended to study iodine speciation as a function of pressure, with calculations performed at 0.2 and 10 MPa steam, and at 10 MPa hydrogen-steam. No figures are provided for these calculations as the results are very similar to those presented in Sec. III.D. The chemical compounds are treated as behaving ideally, with no thermodynamic property dependence on pressure, which is a reasonable approximation even for pressures up to 10 MPa. The main effect of the pressure on the speciation of these compounds will be to determine the absolute number of moles of each element included in the calculation, with the concentration in the coolant increasing with decreasing pressure.

The results of the pressure dependence calculations show that the mole fraction of volatile iodine remains well below 0.1% at 1000 K.

III.F. Role of Other Fission Products, Fuel, and Additives in Iodine Chemistry

Whether determined by thermodynamic or kinetic considerations, iodine speciation will be governed by the chemical environment, which includes other fission product compounds. In particular, the fission products tellurium and molybdenum are of interest, being both abundant and potentially volatile under LOCA-LOECC conditions, and having the ability to combine with cesium to form cesium telluride and cesium molybdate, thereby reducing the amount that is able to combine with iodine. Typical mole ratios in CANDU fuel at discharge burnup are cesium-to-iodine = 9.4, cesium-to-tellurium = 5.3, and cesium-to-molybdenum = 0.63 [derived from values in Table IV (Ref. 39)].

Chemical thermodynamic calculations have been expanded to include tellurium, molybdenum, and uranium along with the cesium and iodine. Thermal-hydraulic conditions were chosen to be the same as those used in the calculations of the cesium-iodine and steam-hydrogen systems discussed earlier (pressure of 1.2 MPa, in pure steam, 50%/50% steam-hydrogen mixture) and were extended to include 100% H_2 .

III.F.1. Tellurium

The calculations indicated that the presence of tellurium had very little effect on iodine speciation, which formed CsI in both pure H_2 and pure H_2O . Cesium telluride compounds, $\text{Cs}_2\text{Te}_3(\text{s})$ and $\text{Cs}_2\text{Te}(\text{c})$, were formed, but these did not destabilize the CsI. Tellurium has a lower molar inventory than Cs and a similar or slower percentage release rate, so it is not likely to become a significant factor regarding iodine volatility. If tellurium is going to have a significant impact on iodine release, it will likely arise from interactions in the aqueous environment of the sump, rather than in release from the HTS.²⁴ The water chemistry of tellurium will be strongly

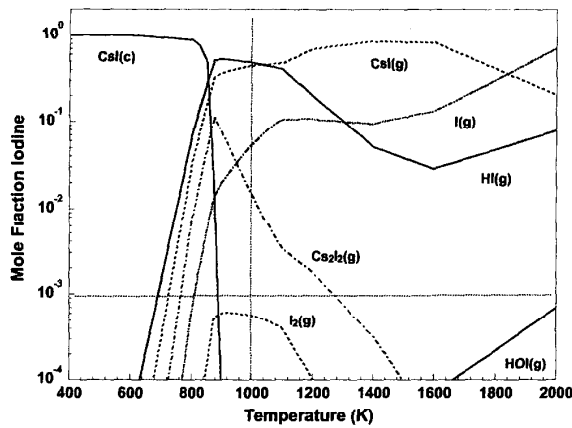


Fig. 7. Mole fraction of iodine as a function of temperature (K). Thermodynamic equilibrium calculations were performed assuming standard conditions, or an iodine-to-steam mole ratio of 2.5×10^{-5} and a total pressure of 1.2 MPa. The cesium-to-iodine ratio was 10. Molybdenum was also included in the calculation with a cesium-to-molybdenum ratio of 1:1. Condensed phase is designated as (c). Other species are in the gas phase.

dependent on pH and radiolysis, an area of research not explored in detail in this paper.

III.F.2. Molybdenum

Molybdenum is of particular concern for certain accident scenarios. Cesium molybdates are thermodynamically more stable than other molybdenum or other cesium species. Fission product molybdenum has the potential to form cesium molybdate [Cs₂MoO₄(c)], which may act as a cesium sink under some circumstances. Because molybdenum has a greater molar inventory than cesium, by a factor of ~2, molybdenum has the potential to consume a significant quantity of cesium, particularly under oxidizing conditions. Under these conditions, the relative ratio of cesium to iodine in the HTS could be significantly reduced. Sensitivity to a reduction in this ratio was discussed in Sec. III.B. In this section, additional calculations were performed for cases with molybdenum species added to the database. The amount of molybdenum added to the system was such that the cesium-to-molybdenum mole ratio ranged from 1 to 1000. These values are well below those predicted by the CORSOR estimate^f of a cesium-to-molybdenum mole ratio of 2×10^5 and were chosen to simulate a worst-case scenario situation.

The calculations presented in Fig. 7 show the effect on iodine speciation if molybdenum is included with a

^fMolybdenum release under neutral or reducing conditions was assumed to be equivalent to uranium release.

cesium-to-molybdenum ratio of 1 in steam atmosphere. Under these conditions, Cs₂MoO₄(c) becomes an important cesium species, and volatile forms of iodine [notably HI(g) and I(g)] are produced at much lower temperatures than in the calculations without molybdenum (Fig. 2). The participation of molybdenum in cesium chemistry is demonstrated in the comparison of Figs. 3 and 7, with molybdenum effectively lowering the free cesium-to-iodine ratio in the calculation for Fig. 7. In both Figs. 3 and 7, the yield of HI(g) and I(g) is increased at 1000 K although the absolute values of these volatile components is different in Figs. 3 and 7.

The presence of molybdenum in the HTS can have a significant impact on the volatile iodine fraction because Cs₂MoO₄(c) is more stable than CsI(c) at oxygen potentials [$RT \ln(pO_2)$] greater than $-400 \text{ kJ} \cdot \text{mol}^{-1}$ at 1000 K (Table V). The oxygen potential of the system shown in Fig. 7 at 1000 K is $-265 \text{ kJ} \cdot \text{mol}^{-1}$. At this oxygen potential, cesium would react with molybdenum preferentially over iodine. However, as long as sufficient cesium remains to react with iodine following reaction with molybdenum, the volatile iodine fraction would be as small as shown for the calculations with no molybdenum. Thermodynamic calculations indicate that when the cesium-to-molybdenum ratio is >2.5 , the mole fraction of volatile iodine is $<0.1\%$. A graph of these results is not included in this paper as there is little difference compared with the speciation shown in Fig. 2. The release behavior of molybdenum from fuel into the HTS, in relation to that of cesium and iodine, will determine the relative ratio of cesium, iodine, and molybdenum as a function of time in the HTS and is thus very important in determining the volatile iodine fraction.

The calculations with molybdenum also served to check whether a reduction in the cesium-to-iodine ratio

TABLE V
Gibbs Energy of Reaction to Form Cs₂MoO₄ and CsI as Functions of Oxygen Potential at 1000 K (Ref. 8)

$\Delta_r G(T, p(O_2))$ (kJ·mol ⁻¹) 2Cs(g) + Mo(c) + 2O ₂ (g) = Cs ₂ MoO ₄ (c)	$\Delta_f G^\circ$ CsI (kJ·mol ⁻¹)	$RT \ln(p(O_2)/\text{bar})$ kJ·mol ⁻¹
96	-230	-500
-196	-230	-400
-396	-230	(intact irradiated fuel) -300
-596	-230	-200
-796	-230	-100
-996	-230	(-13 = air at 1000 K) 0 (1 bar = 0.1 MPa— thermodynamic standard state)

used in Sec. III.B accurately represents the effect of additional fission product interactions. The comparisons of the predicted CsI and volatile iodine [HI(g) + I(g)] for calculations with a cesium-to-iodine ratio of 1:1 and a cesium-to-molybdenum content of 2.22 (which should yield comparable amounts of free cesium) are shown in Fig. 8.

The results of the calculations with a cesium-to-iodine ratio of 1 and a cesium-to-molybdenum ratio of 2.22 show similar trends. The main difference between the two calculations is that the former shows a mole fraction of volatile iodine of 3% at 1000 K, and the latter shows a mole fraction of 1%. In sampling cesium-to-molybdenum ratios in this region, it was discovered that the chemical thermodynamic calculations are extremely sensitive to small changes in the amount of molybdenum present. For instance, if the cesium-to-molybdenum ratio is 2.5, then the mole fraction of volatile iodine is 0.1%. If it is 2.20, then the mole fraction of volatile iodine is 15%. In this context, the results of the calculations presented in Fig. 8 are in good agreement. For accident analysis, this result indicates that emphasis should be placed on a good estimate of the cesium-to-molybdenum mole ratio.

III.F.3. Uranium

Uranium release is expected to be a small fraction of the gap inventory of fission products. However, there are scenarios when elevated local concentrations of uranium could occur, for instance, in the interaction of fission

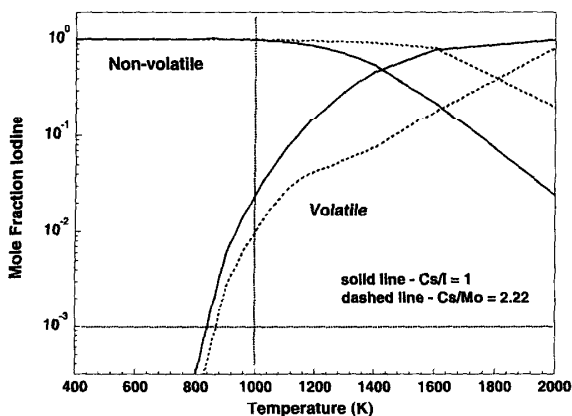


Fig. 8. Fraction of volatile and nonvolatile iodine as a function of temperature (K). The dashed lines were calculated in a system with molybdenum, and the solid lines were calculated with a reduced cesium-to-iodine ratio. The nonvolatile fraction includes CsI in various forms, and the volatile fraction includes HI and I atom. Calculations were performed in 4 mol steam at 1.2 MPa.

products with uranium-bearing aerosols in the HTS. Hence, calculations were performed with uranium in the system, with a uranium-to-cesium ratio of 1.

The iodine speciation above the cesium-uranium system was very similar to that observed under standard conditions (a cesium-to-iodine ratio of 10, an iodine-to-steam ratio of 2.5×10^{-5} , and a pressure of 1.2 MPa). Although $\text{Cs}_2\text{UO}_4(\text{s})$ was the dominant cesium species up to 1050 K, the main iodine species was $\text{CsI}(\text{g})$ at 1000 K. The mole fraction of volatile iodine at 1000 K was 2×10^{-4} . At 1050 K, $\text{Cs}_2\text{U}_4\text{O}_{12}(\text{s})$ became the main cesium species. However, $\text{CsI}(\text{g})$, $\text{Cs}_2\text{UO}_4(\text{s})$, and $\text{CsOH}(\text{g})$ were also important. When heated to higher temperatures, the cesium uranates decomposed, releasing cesium, and were not found in the vapor phase in the fuel channel.³³ Hence, the amount of $\text{Cs}_2\text{UO}_4(\text{s})$ was reduced above 1050 K, with the mono-uranate disappearing completely by 1200 K. $\text{Cs}_2\text{U}_4\text{O}_{12}(\text{s})$ disappeared by 2000 K.

Simulations were also run with a combination of uranium and molybdenum to investigate whether they would work in concert to destabilize CsI in steam at high temperatures. The mole ratios of cesium-molybdenum-uranium were all 1:1:1, with the cesium-to-iodine ratio being 10. The results of the simulation showed little change in cesium chemistry from the cesium-molybdenum system because uranates were not formed nor was the iodine speciation significantly different from the cesium-molybdenum system. Hence, the presence of uranium has little effect on the speciation of iodine or cesium in the presence of molybdenum in steam.

III.F.4. Lithium

Lithium hydroxide (up to 3.6 mol ppm of lithium) is added to CANDU cooling water for pH control. At the high temperatures expected in the channel for a LOCA-LOECC scenario, lithium will be vaporized along with the coolant. Lithium iodide is slightly less stable than CsI but has melting and boiling points that are similar to those of CsI (for LiI, 716 and 1443 K, respectively; for CsI, 894 and 1553 K, respectively).⁴⁰ Lithium will probably react with many compounds and surfaces that react with cesium; therefore, the presence of lithium will tend to reduce iodine volatility. The lowering of the mole fraction of volatile iodine will be particularly important at low fission product-to-steam ratios, giving a lower bound to the concentration of available cation in the coolant. The mitigating effect of lithium has not been included in these calculations because the lithium concentration is not very well defined in the case of partial emergency core cooling injection.

In addition to salts of lithium, rubidium, and bromine are fission products that react very similarly to cesium and iodine, respectively. The fission yield ratios are cesium-to-iodine = 10, cesium-to-rubidium = 5, and iodine-to-bromine = 7; thus, the overall effect on CsI stability is not expected to be dramatic.

III.G. Summary

Thermodynamic equilibrium calculations were used to model iodine speciation in the HTS under LOCA-LOECC conditions, low steam flows, and high fuel temperatures. The major iodine species that can be formed in the fuel and the HTS are CsI, Cs₂I₂, HI, HOI, I, and I₂. The volatile iodine species, which include I, I₂, HI, and HOI, are of particular interest in safety analysis, as they would be gaseous under the low-temperature containment conditions. However, hydrogen iodide that can be formed at low cesium-to-molybdenum ratios (<2.5) is very water soluble⁴¹ and should be quickly dissolved in water once it is released into containment. Volatile atomic iodine and HOI are not thermodynamically stable in the containment environment following an accident and furthermore would dissolve in water or react with ozone (produced in the radiolysis of air) to form solid iodine oxides. Therefore, the assumption that HI, HOI, and I released from the HTS would remain in containment in volatile form is probably conservative.

Because of the possibility that the omission of certain elements and species may affect the cesium and iodine speciation and because of uncertainties in the level of these elements (particularly molybdenum), a sensitivity analysis was performed, varying the amount of fission products released from fuel and the thermal-hydraulic conditions. Thermodynamic equilibrium calculations were performed for conditions and cesium-to-iodine ratios much different from those expected in the HTS following a postulated accident. It was found that the fraction of volatile iodine increases with

1. a decrease in the cesium-to-iodine ratio
2. a decrease in iodine concentration in the coolant
3. an increase in oxygen partial pressure.

Among the parameters studied, the mole fraction of volatile iodine was most sensitive to the cesium-to-iodine ratio and somewhat sensitive to the iodine-to-steam ratio.

The impact of other fission products that may react with cesium and thus could effectively reduce the cesium-to-iodine ratio was also examined using chemical equilibrium calculations. It was determined that since CsI is very stable, it will not react with many fission products, such as tellurium. Molybdenum release has the potential to alter calculated iodine speciation significantly. Molybdenum and uranium are examples of elements that can destabilize CsI, allowing the formation of Cs₂MoO₄ and cesium uranate [i.e., Cs₂UO₄(s), Cs₂U₂O₇(s), or Cs₂U₄O₁₂(s)], respectively. The uranates can form in the fuel under localized oxidizing conditions. However, for these calculations where the release from the fuel has already occurred, the effect of uranium on iodine chemistry was found to be insignificant compared to that of molybdenum.

IV. CONCLUSIONS

Chemical thermodynamic equilibrium calculations were used to test the assumption that the theoretical mole fraction of volatile iodine that would be released from the HTS into containment would be <0.1% in a severe accident (i.e., LOCA-LOECC) involving complete vaporization of the coolant in a CANDU channel with sufficient H₂O to perpetuate the Zircaloy-water reaction. This was found to be the case under reference conditions that predicted iodine to be predominantly in the form of CsI at 1000 K. Downstream, in containment where temperatures will be <425 K, cesium iodide is solid and will be transported in water-droplet aerosols, whereas all the other iodine species could remain as gases and thus are included in determining the volatile fraction.

Sensitivity studies of the chemical thermodynamic system showed that when the concentration of CsI in steam is 100 times lower than the maximum estimated using CORSOR correlations, the mole fraction of iodine entering containment in volatile form may exceed 0.1%. This upper bound for the mole fraction of volatile iodine, however, was established in consideration of the maximum release rate of cesium and iodine into containment. So, it is likely that situations involving lower concentrations of released cesium and iodine in the primary coolant will occur with a lower overall release to containment.

Molybdenum can affect iodine chemistry depending on the oxygen partial pressure in the channel. The conclusions of the Knudsen-cell experiments, backed up by thermodynamic calculations, were that the reaction of CsI with elemental molybdenum is unlikely to be a major contributor to molybdate formation, even in the presence of slightly hyperstoichiometric fuel. However, cesium molybdate is readily formed at higher oxygen potentials, such as in the presence of MoO₃, suggesting a role for the ternary compound in an accident involving oxidizing conditions.

Chemical speciation is complex but is a key element in understanding the transport of fission products into containment. In the work described in this paper, chemical thermodynamic calculations were used to model the chemical behavior of iodine and other fission products in the HTS. The CHMWRK code and its thermodynamic database were used to address questions of a chemical nature that have arisen as a result of CANDU safety and licensing issues.

ACKNOWLEDGMENTS

The authors thank the members of the Fission Product Release and Transport Safety Analysis Methodologies team: Z. Liu and L. W. Dickson, at Atomic Energy of Canada Limited, for their helpful discussions and suggestions concerning fission product behavior, as well as K. Weaver, at Ontario Power Generation, and D. Bowslaugh, M. Cormier, and R. Khaloo, at Atomic Energy of Canada Limited, for sharing their expertise

on accident methodologies. The work of J. C. LeBlanc in collecting Knudsen-cell data, F. Garisto in development of the CHMWRK code, and D. J. Wren in the chemical kinetic analysis of iodine chemistry in the CANDU fuel channel laid the foundation for the analyses reported here. The authors thank S. Sunder, S. Stroes-Gascoyne, and W. M. Collins for their helpful discussions and for reviewing the paper.

REFERENCES

1. C. E. L. HUNT, F. C. IGLESIAS, and D. S. COX, "Measured Release Kinetics of Iodine and Cesium from UO_2 at High Temperatures Under Reactor Conditions," *Fission Product Transport Processes in Reactor Accidents*, p. 163, J. T. ROGERS, Ed., Hemisphere Publishing, New York (1989).
2. D. J. WREN, "Kinetics of Iodine and Cesium Reactions in the CANDU Reactor Primary Heat Transport System Under Reactor Accident Conditions," AECL-7781, Atomic Energy of Canada Limited, Whiteshell Nuclear Research Establishment (1983).
3. E. C. BEAHM, C. F. WEBER, T. S. KRESS, and G. W. PARKER, "Iodine Chemical Forms in LWR Severe Accidents," NUREG/CR-5732, ORNL/TM-11861, Oak Ridge National Laboratory (1992).
4. F. GARISTO, "Thermodynamics of Iodine, Cesium and Tellurium in the Primary Heat-Transport System Under Accident Conditions," AECL-7782, Atomic Energy of Canada Limited, Whiteshell Nuclear Research Establishment (1982).
5. J. McFARLANE, J. C. LeBLANC, and D. G. OWEN, "High-Temperature Chemistry of Molybdenum, Cesium, Iodine and UO_{2+x} ," AECL-11708, Atomic Energy of Canada Limited Report, Whiteshell Laboratories (1996).
6. D. JACQUEMAIN, N. HANNIET, C. POLETIKO, S. DICKINSON, C. WREN, D. A. POWER, E. KRAUSMANN, F. FUNKE, R. CRIPPS, and B. HERRERO, "An Overview of the Iodine Behaviour in the Two First PHEBUS Tests FPT 0 and FPT-1," *Proc. OECD Workshop on Iodine Aspects of Severe Accident Management*, NEA/CSNI/R(99)7, p. 79, Nuclear Energy Agency Committee on the Safety of Nuclear Installations (1999).
7. W. R. SMITH and R. W. MISSEN, *Chemical Reaction Equilibrium Analysis: Theory and Algorithms*, John Wiley and Sons, New York (1982).
8. E. H. P. CORDFUNKE and R. J. M. KONINGS, Eds., *Thermochemical Data for Reactor Materials and Fission Products*, North Holland, Amsterdam (1990).
9. J. D. COX, D. D. WAGMAN, and V. A. MEDVEDEV, *CODATA Key Values for Thermodynamics*, Hemisphere Publishing Corporation, New York (1988).
10. L. V. GURVICH, I. V. VEYTS, and C. B. ALCOCK, *Thermodynamic Properties of Individual Substances*, Vol. 1, 4th ed., Hemisphere Publishing Corporation, New York (1989).
11. E. H. P. CORDFUNKE, R. J. M. KONINGS, and S. R. M. MEYSSSEN, "Vapour Pressures of Some Caesium Compounds. II. Cs_2MoO_4 and Cs_2RuO_4 ," *J. Chem. Thermodyn.*, **24**, 725 (1992).
12. V. P. GLUSHKO, L. V. GURVICH, G. A. BERGMAN, I. V. VEYTS, V. A. MEDVEDEV, G. A. KHACHURUZOV, and V. S. YUNGMAN, Eds., *Termodinamicheskie Sovistva Individual'nykh Veshchestv*, Vol. 4, Nauka, Moscow (1982).
13. R. H. LAMOREAUX and D. L. HILDENBRAND, "High Temperature Vaporization Behavior of Oxides. I. Alkali Metal Binary Oxides," *J. Phys. Chem. Ref. Data*, **13**, 151 (1984).
14. S. P. BERARDINELLI, Sr., and D. L. KRAUS, "Thermal Decomposition of the Higher Oxides of Cesium in the Temperature Range 320-500°," *Inorg. Chem.*, **13**, 189 (1974).
15. M. W. CHASE, "NIST-JANAF Thermochemical Tables for the Iodine Oxides," *J. Phys. Chem. Ref. Data*, **25**, 1298 (1996).
16. Y. BEDJANIAN, G. LE BRAS, and G. POULET, "Kinetics and Mechanism of the $IO + ClO$ Reaction," *J. Phys. Chem.*, **101**, 4088 (1997).
17. F. GARISTO, "Ideal Gas Thermodynamic Properties of Hypoiodous Acid," *Thermochim. Acta*, **63**, 251 (1983).
18. Z. ZHANG, P. S. MONKS, L. J. STIEF, J. F. LIEBMAN, R. E. HUIE, S.-C. KUO, and R. B. KLEMM, "Experimental Determination of the Ionization Energy of $IO(X^2\Pi_{3/2})$ and Estimations of $\Delta_f H_0^\circ(IO)$ and $PA(IO)$," *J. Phys. Chem.*, **100**, 63 (1996).
19. L. V. GURVICH, G. A. BERGMAN, L. N. GOROKHOV, V. S. IORISH, V. Ya. LEONIDOV, and V. S. YUNGMAN, "Thermodynamic Properties of Alkali Metal Hydroxides. Part II. Potassium, Rubidium, and Cesium Hydroxides," *J. Phys. Chem. Ref. Data*, **26**, 1031 (1997).
20. L. B. PANKRATZ, *Thermodynamic Properties of Elements and Oxides*, Bulletin 672, U.S. Department of the Interior, Bureau of Mines (1982).
21. K. C. MILLS, *Thermodynamic Data for Inorganic Sulphides, Selenides, Tellurides*, Butterworth, London (1974).
22. D. W. MUENOW, J. W. HASTIE, R. HAUGE, R. BAUTISTA, and J. L. MARGRAVE, "Vaporization Thermodynamics and Structures of Species in the Tellurium-Oxygen System," *Trans. Faraday Soc.*, **65**, 3210 (1969).
23. H. OPPERMANN, G. KUNZE, E. WOLF, G. A. KOKOVIN, I. M. SITSCHOVA, and G. E. OSIPOVA, "Untersuchungen zum System $Te/O/I$," *Z. Anorg. Allg. Chem.*, **461**, 165 (1980).
24. J. McFARLANE, "Fission Product Tellurium Chemistry from Fuel to Containment," *Proc. OECD/CSNI Workshop on the Chemistry of Iodine in Reactor Safety*, Würenlingen, Switzerland, June 10-12, 1996, p. 563, Organization for Economic Cooperation and Development/Committee on the Safety of Nuclear Installations (1996).

25. E. A. FISHER, "Evaluation of the Urania Equation of State Based on Recent Vapor Pressure Measurements," KfK 4084, Kernforschungszentrum Karlsruhe, Germany (1987).
26. E. A. FISHER, "A New Evaluation of the Urania Equation of State Based on Recent Vapor Pressure Measurements," *Nucl. Sci. Eng.*, **101**, 97 (1989).
27. F. GARISTO, Personal Communication (1993).
28. T. B. LINDEMER and T. M. BESMANN, "Chemical Thermodynamic Representation of $(\text{UO}_{2\pm x})$," *J. Nucl. Mater.*, **130**, 473 (1985).
29. T. B. LINDEMER, T. M. BESMANN, and C. E. JOHNSON, "Thermodynamic Review and Calculations—Alkali Metal Oxide Systems with Nuclear Fuels, Fission Products and Structural Materials," *J. Nucl. Mater.*, **100**, 178 (1981).
30. T. S. L. NARASIMHAN, R. BALASUBRAMANIAN, S. NALINI, and M. S. BABA, "Vaporization Studies on Tellurium Dioxide. A Knudsen Effusion Mass Spectrometric Study," *J. Nucl. Mater.*, **247**, 28 (1997).
31. R. G. J. BALL, B. R. BOWSHER, E. H. P. CORDFUNKE, S. DICKINSON, R. J. M. KONINGS, and M. H. RAND, "Thermochemical Data Acquisition," AEA-TRS-5068 (Jan. 1991).
32. J. McFARLANE, J. C. LeBLANC, and D. G. OWEN, "Sensitivity of Cesium Chemistry to the O/U Ratio in UO_{2+x} ," *Proc. 4th Int. Conf. CANDU Fuel*, Pembroke, Ontario, October 1–4, 1995, Canadian Nuclear Society.
33. J. McFARLANE and J. C. LeBLANC, "High-Temperature Knudsen Cell Studies of the Cesium Iodide in Hyperstoichiometric Uranium Dioxide," *J. Nucl. Mater.*, **256**, 145 (1998).
34. M. R. KUHLMAN, D. I. LEHMICKE, and R. O. MEYER, "CORSOR User's Manual," NUREG/CR-4173, BMI02122 (Mar. 1985).
35. S. R. MULPURU, *Proc. 14th Annual Nuclear Simulation Symp.*, Pinawa, Manitoba, Canada, 1988.
36. R. HOPPE, H. J. ROEHRBORN, and H. WALKER, "New Plumbates and Stannates of Alkali Metals," *Naturwissenschaften*, **51**, 86 (1964).
37. R. M. BRAUN and R. HOPPE, "Oxostannates (ii). Study of Cesium Oxostannate ($\text{Cs}_2\text{Sn}_2\text{O}_3$)," *Z. Anorg. Allg. Chem.*, **480**, 81 (1981).
38. K. UNE, "Reactions of Cesium with Nonstoichiometric UO_{2+x} and $\text{U}_{0.86}\text{Gd}_{0.18}\text{U}_{2+x}$ Pellets," *J. Nucl. Mater.*, **144**, 128 (1987).
39. J. C. TAIT, I. C. GAULD, and G. B. WILKIN, "Derivation of Initial Radionuclide Inventories for the Safety Assessment of the Disposal of Used CANDU Fuel," AECL-9881, Atomic Energy of Canada Limited (1989).
40. V. V. KAFAROV, I. N. DOROKHOV, V. N. VETOKHIN, and L. P. VOLKOV, "Analysis of Physicochemical Properties of Alkali Metal Halides," Academy of Sciences of the USSR, *Dokl. Phys. Chem.*, **312**, 497 (1990). Translated from *Dokl. Akad. Nauk SSSR*, **312**, 1169 (1990).
41. J. McFARLANE and M. HOGEVEEN UNGURIAN, "Droplet Formation in a High Enthalpy Steam Jet," *Proc. 8th Int. Conf. Liquid Atomization and Spray Systems*, Pasadena, California, July 2000.
42. R. P. TANGRI, V. VENUGOPAL, D. K. BOSE, and M. SUNDARFSAN, "Thermodynamics of Vaporization of Cesium Molybdate," *J. Nucl. Mater.*, **167**, 127 (1989).
43. M. YAMAWAKI, T. OKA, M. YASUMOTO, and H. SAKURAI, "Thermodynamics of Vaporization of Cesium Molybdate by Means of Mass Spectroscopy," *J. Nucl. Mater.*, **201**, 257 (1993).

Joanna McFarlane (BSc, chemistry, McGill University, Canada, 1983; PhD, chemistry, University of Toronto, Canada, 1990) works for UT-Battelle at Oak Ridge National Laboratory. She worked at Atomic Energy of Canada Limited (AECL) Whiteshell Laboratories from 1989 to 2001. Her research interests include physical measurements on inorganic and organic compounds, chemical thermodynamic and chemical kinetic modeling, and aerosol physics.

Jungsook Clara Wren (BS, chemistry, Sogang University, Korea, 1976; PhD, physical chemistry, Kansas State University, 1981) is a senior research scientist in the Fuel Safety Branch at the Chalk River Laboratories of AECL. Her background in nuclear safety research includes the reaction kinetics of iodine species in gas and aqueous phases, iodine surface chemistry, and the abatement of iodine and noble gases. Her other research interests include chemical reactions in high-voltage discharges and radiation fields, and intermolecular and intramolecular energy transfer of highly excited molecules.

Robert J. Lemire (PhD, chemistry, University of Toronto, Canada, 1975) works in the Fuel Safety Branch at the Chalk River Laboratories of AECL. His interests include development of chemical thermodynamic databases and the applicability of such databases to reactor-safety computer codes, actinide chemistry, and aqueous solution chemistry of inorganic species.